Dynamics of excitation pulses with attractive interaction: Kinematic analysis and chemical wave experiments

Niklas Manz and Oliver Steinbock*
Department of Chemistry and Biochemistry, Florida State University, Tallahassee, Florida 32306-4390, USA
(Received 10 August 2004; published 22 December 2004)

We present a theoretical analysis of stacking and destacking wave trains in excitable reaction-diffusion systems with anomalous velocity-wavelength dependence. For linearized dispersion relations, kinematic analysis yields an analytical function that rigorously describes front trajectories. The corresponding accelerations have exactly one extremum that slowly decays with increasing pulse number. For subsequent pulses these maxima occur with a lag time equal to the inverse slope of the linearized dispersion curve. These findings are reproduced in experiments with chemical waves in the 1,4-cyclohexanedione Belousov-Zhabotinsky reaction but should be also applicable to step bunching on crystal surfaces and certain traffic phenomena.

DOI: 10.1103/PhysRevE.70.066213 PACS number(s): 05.45.−a, 82.40.Ck, 82.20.Wt

I. INTRODUCTION

Propagating excitation waves exist in a variety of spatially extended, nonlinear systems [1]. Classic examples are traveling action potentials in gastric [2], neuronal [3], and cardiac tissue [4], intracellular Ca^{2+} waves in *Xenopus laevis* oocytes [5], and chemical waves in reaction-diffusion media. The latter class of systems is extremely diverse and includes various liquid-phase reactions [6], catalytic surfaces [7], aggregating cell colonies [8], electrochemical systems [9], yeast extracts [10], single cells [11], as well as the skin of certain hairless mice that shows traveling stripes of different color [12]. Waves in these systems are typically modeled by coupled reaction-diffusion equations that describe the spatiotemporal evolution of two or more chemical species [13]. Numerical integration of such models can yield quantitative information on various features such as pulse velocities and pulse profiles. In many cases, one finds that the pulse profiles are constant with characteristic steep fronts and shallow backs. This feature suggests an alternative description that reduces the problem of analyzing the dynamics of the entire wave pattern to a purely kinematic analysis of the corresponding front curves [14].

In excitable systems with only one spatial dimension, the latter approach represents each wave pulse as a simple, particlelike object. The state of the system is therefore fully determined by the coordinates of the individual particles. To analyze the dynamics of a given system, we need to have knowledge of the rules that govern the repulsive and/or attractive particle-particle interaction. In most experimental reaction-diffusion systems, this interaction is described by the underlying dispersion relation which quantifies the dependence of pulse speed on interpulse distance [15]. The dispersion curve reflects the response of the propagating pulse to the refractory tail of its immediate predecessor. For example, monotonic decay of an inhibitory species within the refractory tail gradually increases the speed of the trailing pulse as it is separated farther from its predecessor.

Most experimental systems follow the latter scenario and obey normal dispersion relations for which the propagation speed increases monotonically while converging to a finite maximal value for large interpulse distances [16]. In recent years, however, at least three reactions have been identified that show anomalous behavior, namely, the catalytic reduction of NO with CO on a Pt(100) surface [17], the Belousov-Zhabotinsky system dispersed in a water-in-oil microemulsion (BZ-AOT system) [18], and the 1,4-cyclohexanedione Belousov-Zhabotinsky (CHD-BZ) reaction [19]. In these systems, trailing pulses can be attracted by their leading counterparts indicating that the underlying dispersion curve has a negative slope over a large range of interpulse distances. For the CHD-BZ reaction, this anomalous dispersion relation has been measured quantitatively [20], revealing nonmonotonic dependencies similar to the solid curve in Fig. 1. Similar anomalous behavior can be found also in neuronal systems [21], where it is referred to as "supernormal excitability," and possibly in aggregating populations of the widely studied social amoeba *Dictyostelium discoideum* [22].

Recent investigations of the CHD-BZ reaction show a variety of interesting pulse dynamics [19,20,23]. Foremost, one

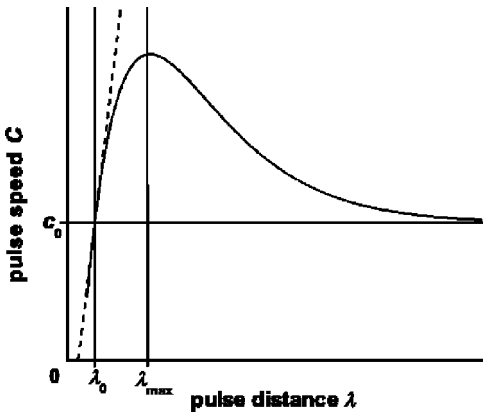

FIG. 1. Schematic drawing of an anomalous dispersion relation (solid curve). At the interpulse distance λ_0 the pulse speed C equals the speed c_0 of solitary fronts. The dashed line is the linear approximation of the dispersion curve at the point λ_0.

*Electronic address: steinbck@chem.fsu.edu

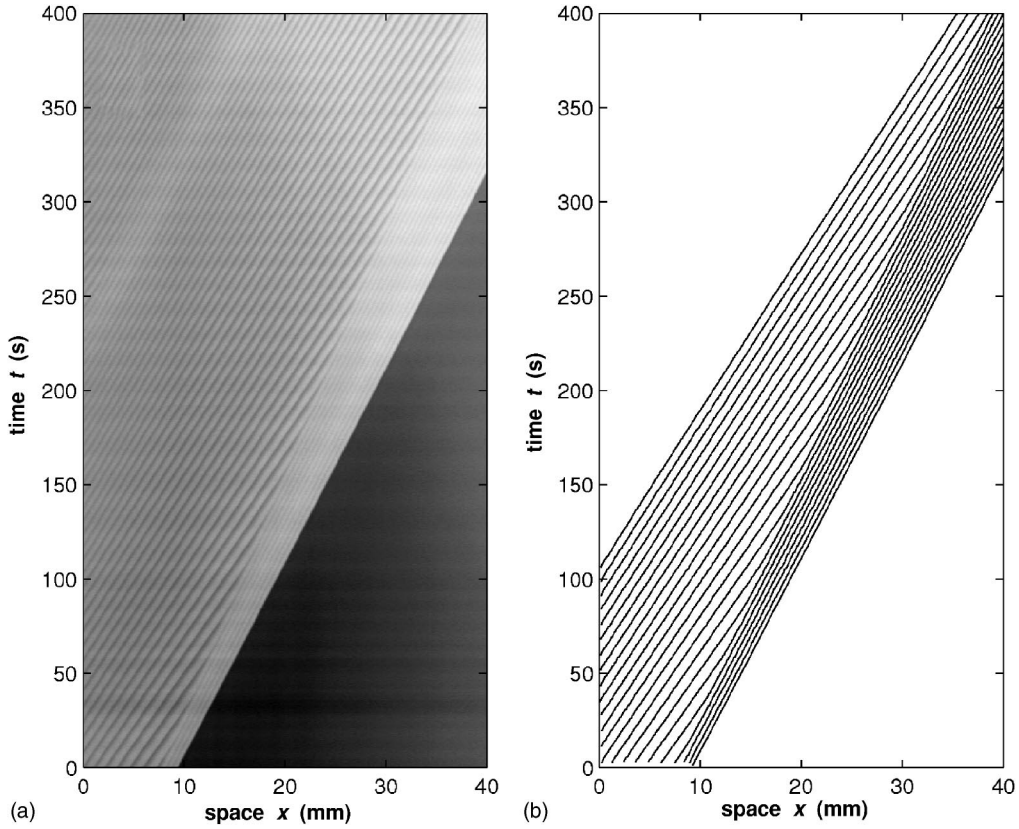

FIG. 2. (a) Space-time plot obtained from absorption profiles of the experimental system. (b) Space-time trajectories of the first 23 pulse fronts. The values for λ_0 and c_0 of the stacked pulses are 0.525 mm and 0.097 mm/s, respectively. Initial concentrations: $[H_2SO_4]=2.0$ M, [CHD]=0.2 M, $[NaBrO_3]=0.14$ M, and [ferroin]=0.5 mM.

observes that pulses in finite wave trains stack in the wake of their leading pulse at a characteristic interpulse distance λ_0. This phenomenon is similar to a traffic jam in which fast moving cars decelerate as they approach a slow moving vehicle [24]. As illustrated in Fig. 1, the distance λ_0 is determined by the speed c_0 of the slow frontier pulse and the condition $C(\lambda_0)=c_0$. The resulting stacked wave train is stable against small perturbation if $dC(\lambda_0)/d\lambda>0$. The dynamics of the deceleration process depends strongly on the initial pulse distance λ and the interpulse distance λ_{max} for which the anomalous dispersion curve reaches a maximum. For $\lambda_0<\lambda<\lambda_{max}$, the deceleration occurs in a shocklike fashion [25] and the "compression point" moves with a constant velocity [26].

A typical example of this stacking dynamics in a quasi-one-dimensional, ferroin-catalyzed CHD-BZ system, performed in a capillary, is shown in Fig. 2. The plot in Fig. 2(a) is generated by piling up consecutive absorbtion profiles of the pseudo-one-dimensional reaction medium. In this representation, each oxidation pulse generates a bright band within the space-time plot while the reduced medium appears dark. The slope of these bands equals the inverse propagation velocity. Figure 2(b) shows the space-time trajectories of the first 23 pulses in Fig. 2(a) and clearly reveals the slow moving compression point.

For $\lambda>\lambda_{max}$, the wave train undergoes cascades of "bunching" events and forms clusters of closely spaced, nearly stable pulses that are separated by large, and hence less unstable, distances [27]. In the case $\lambda<\lambda_0$, for which the wave train is initially very dense, one finds a successive destacking of the structure that quickly establishes the stable stacked pattern of interpulse distance λ_0.

The dynamic phenomena of pulse stacking and bunching can be reproduced by numerical simulations of the underlying reaction-diffusion equations and have also been analyzed in terms of the corresponding ordinary differential equations that one obtains in co-moving coordinate systems. Here, we present a rigorous kinematic analysis of pulse stacking and destacking for linearized dispersion curves that yields analytical expressions for all pulse trajectories. Moreover, these findings are compared to results obtained from experiments with the CHD-BZ reaction.

II. EXPERIMENT

Our experiments employ the ferroin-catalyzed Belousov-Zhabotinsky reaction using 1,4-cyclohexanedione as the organic substrate [28]. Aqueous stock solutions of 2.0 M sodium bromate (Fluka) and 0.5 M 1,4-cyclohexanedione (Aldrich) are prepared in nanopure water (18 MΩ cm) obtained from a Barnstead EASYpure UV unit. CHD solution is filtered through a Whatman 0.2 μm nylon filter. Ferroin (25 mM, Fluka) and sulfuric acid (5 M, Riedel–de Haën) are purchased as standardized solutions and used without further purification.

All experiments are carried out in thin capillaries with an inner diameter of 0.63 mm and a length of 64 mm (Drummond 20 μL MICROCAPS). Absorption profiles are monitored with a monochrome charge-coupled-device camera (COHU 2122; 640×480 pixel, 8 bit per pixel). The video signal is digitized with a low-noise image-acquisition card (Data Translation DT3155). Image data are acquired every 0.5 s as bitmap frames using commercial software (HLImage++97). For image analysis we use programs written in IDL (Interactive Data Language, Research System Inc., Versions 5.2). All experiments are performed at (24 ± 1) °C.

III. THEORETICAL ANALYSIS

As outlined in the Introduction, kinematic descriptions of excitation waves focus on the dynamics of the individual pulse fronts rather then the analysis of the entire wave pattern. Such approaches have been employed successfully for the description of rotating spiral waves and other stationary and/or transient structures [29]. Our discussion is strictly limited to the kinematic analysis of one-dimensional systems. In this case, the dynamics of a wave train is completely described by the space-time trajectories $x_n(t)$ of each of its pulse fronts. We denote the leading pulse as $n=0$ and assume that its velocity c_0 is constant and positive. Without loss of generality we further assume that its initial position is $x_0(0)=0$. Consequently, the leading pulse is described by $x_0(t)=c_0t$. All subsequent pulses are labeled consecutively as $n=1,2,\ldots$ and their positions at time $t=0$ are denoted as s_n. Since $c_0>0$ and $x_0(0)=0$, the latter values are negative and obey the relation $s_{n-1}>s_n$.

For a given set of initial positions, the evolution of the wave train only depends on the dispersion relation $C(\lambda)$ and can be calculated according to the equation

$$\frac{\mathrm{d}x_n}{\mathrm{d}t}=C(x_{n-1}-x_n) \tag{1}$$

that relates the velocity of the nth pulse $(n>0)$ to the distance $x_{n-1}-x_n$ from its predecessor.

The phenomena of wave stacking and destacking involve interpulse distances λ that differ only slightly from λ_0. We therefore linearize the given dispersion relation around λ_0 and obtain

$$C(\lambda)=c_0+\nu(\lambda-\lambda_0), \tag{2}$$

where ν denotes the slope $\mathrm{d}c/\mathrm{d}\lambda$ of the dispersion curve at λ_0. Using Eq. (2) and the initial conditions specified above, one can solve Eq. (1) rigorously and obtains

$$x_n(t)=c_0t-n\lambda_0+e^{-\nu t}\sum_{i=0}^{n-1}\frac{(\nu t)^i}{i!}[(n-i)\lambda_0+s_{n-i}]. \tag{3}$$

Further analysis requires additional information regarding the experimental conditions that determine the constants s_n. In the following, we consider the case in which at time $t=0$ all pulses are equally spaced. Although similar, this case should be distinguished from a situation in which pulses are generated by a periodic pacemaker at $x=0$. The latter case is more complicated because the pulse velocities at the pacemaker are not constant for small n, which yields cumbersome, recursive expressions for the integration constants s_n. A brief discussion is presented in the Appendix.

If the pulses are equally spaced at time $t=0$, Eq. (3) can be expressed in terms of analytical functions. Let λ denote the initial spacing between next-neighbor pulses. With $s_n=-n\lambda$ $(\lambda>0)$, we find that

$$x_n(t)=c_0t-n\lambda_0+(\lambda-\lambda_0)\frac{(\nu t-n)\Gamma(n,\nu t)-(\nu t)^n e^{-\nu t}}{\Gamma(n)}, \tag{4}$$

where $\Gamma(n)$ and $\Gamma(n,\nu t)$ are the complete and the "upper" incomplete gamma function, respectively. Two typical examples for the dynamics described by Eq. (4) are shown in Fig. 3, where (a) and (b) correspond to pulse stacking $(\lambda>\lambda_0)$ and destacking $(\lambda<\lambda_0)$, respectively. For clarity, the plots are not depicting the nearly linear trajectories for $x<0$.

From Eq. (4), we obtain the velocity v_n and the acceleration a_n of the nth pulse as

$$v_n(t)=c_0+\nu(\lambda-\lambda_0)Q(n,\nu t), \tag{5}$$

$$a_n(t)=-(\lambda-\lambda_0)\frac{\nu^{n+1}t^{n-1}e^{-\nu t}}{\Gamma(n)}, \tag{6}$$

where $Q(n,\nu t)=\Gamma(n,\nu t)/\Gamma(n)$ is the regularized gamma function. The acceleration of the first trailing pulse $(n=1)$ obeys a simple exponential function that rapidly converges to zero as the distance from the frontier pulse approaches λ_0. The acceleration of later pulses $(n>1)$, however, has a local extremum A_n at time τ_n. From Eq. (6) and $\mathrm{d}a_n/\mathrm{d}t=0$, we obtain

$$\tau_n=\frac{n-1}{\nu}, \tag{7}$$

$$A_n=-\nu^2(\lambda-\lambda_0)\frac{(n-1)^{n-1}e^{1-n}}{\Gamma(n)}. \tag{8}$$

Figures 3(c) and 3(d) show examples for the resulting temporal evolution of the pulse acceleration. The plots illustrate the simple, n dependent shift of extrema and decay of amplitude described by Eqs. (7) and (8). Notice that, in the framework of our analysis, stacking wave trains have strictly nonpositive acceleration. However, in cases where the nonlinearity of the dispersion curve becomes relevant (cf., Fig. 1), this result does not hold and one expects pulses to accelerate prior to their insertion into the stacked pulse packet.

IV. EXPERIMENTAL RESULTS

Our theoretical findings are compared to experimental results obtained from chemical waves in the CHD-BZ reaction. This system is similar to the classic Belousov-Zhabotinsky reaction, but it employs 1,4-cyclohexanedione rather than

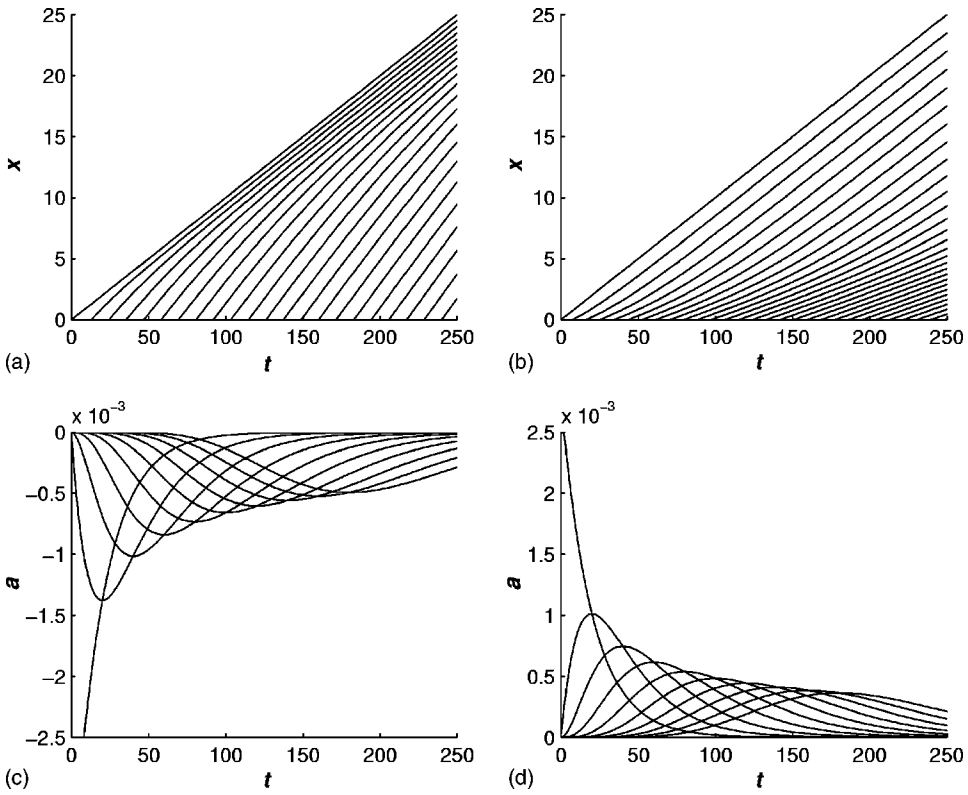

FIG. 3. Temporal evolution of stacking (a), (c) and destacking (b), (d) pulses. The plots show the positions $x(t)$ and accelerations $a(t)$ for numerous consecutive pulses as calculated from Eqs. (4) and (6). The slope of the dispersion curve ν and the velocity of the first pulses c_0 are 0.05 and 0.1, respectively. The initial and the final pulse distances are $\lambda=2.0$ and $\lambda_0=0.5$ (a), (c) and $\lambda=0.4$ and $\lambda_0=1.5$ (b), (d).

malonic acid as its organic substrate. The CHD-BZ reaction forms no gaseous reaction products that could nucleate undesired bubbles [30]. Therefore, it can be readily studied in thin, open glass capillaries that approximate a one-dimensional excitable medium. Under these conditions, waves nucleate spontaneously at the ends of the capillary, where bromine, an inhibitor of the reaction, diffuses from the aqueous phase into the ambient atmosphere.

Figure 4 shows two representative space-time plots of chemical waves in the ferroin-catalyzed CHD-BZ system. In Fig. 4(a), two wave pulses are triggered at both ends of the capillary tubes, whereas in Fig. 4(b) no waves are initiated at the right end. The leading pulses are slower than the trailing fronts, thus, indicating the presence of anomalous dispersion. At $t=0$ s the interpulse distance in Fig. 4(a) ($\lambda=2.5$ mm) is approximately two times smaller than in Fig. 4(b) ($\lambda=5.1$ mm).

A comparison of Figs. 4(a) and 4(b) reveals that the trailing pulses show qualitatively different dynamics. In (a), we observe a simple exponential approach during which the pulse acceleration is strictly negative. Its trajectory, given by Eq. (3), is in very good agreement with the theoretical description (see superimposed solid, black line on the left trailing pulse). In (b), however, the trailing front accelerates during its initial approach of the leading pulse. This behavior results from an initial interpulse distance that is larger than the distance $\lambda_{\max}$ at which the underlying dispersion curve reaches a maximal velocity (cf. Fig. 1). Accordingly, the trailing pulse moves "over the hump" of the dispersion curve, thus undergoing an initial acceleration, which causes wave bunching for larger wave trains. We emphasize that the latter behavior is not captured by our theoretical analysis that relies on a linearized approximation of the normal branch of the dispersion relation.

Using the experimental data in Fig. 2, we compute the acceleration $a_n(t)$ for some of the early, stacking wave pulses [see Fig. 5(a)]. For each pulse, we find exactly one pronounced maximum of deceleration. The height of these maxima decreases with increasing pulse number n. The experimental results shown in Fig. 5(a) are in qualitative agreement with our theoretical analysis that predicts a decrease in the minimum of $a_n(t)$ with increasing values of n (cf. Fig. 3). A quantitative comparison, however, shows that Eq. (6) underestimates the experimental values.

Figure 5(b) shows the time τ_n at which the acceleration of the nth pulse reaches its extremum. The data reveal a linear dependence of peak time on pulse number as predicted by Eq. (7) and shown in Fig. 3. Linear regression yields an inverse slope of 0.042 s^{-1}.

With this experimental value of the slope it is possible to calculate the velocity of the shock point in Fig. 2 and to compare our equations with the relation $c_s=(c_0\lambda_1-c_1\lambda_0)/(\lambda_1-\lambda_0)$. This equation is related to the Rankine-Hugoniot relation [31] and was first used in the context of reaction-diffusion systems to describe collision lines between target patterns [25]. More recently, the applicability of this equation to stacking waves was demonstrated experimentally using the CHD-BZ reaction [26]. In this equation c_0 and c_1 denote the velocities of stacked and fast waves, respectively. Their corresponding wavelengths are given by λ_0 and λ_1. Using the experimental values $c_0=0.097$ mm/s, $c_1=0.127$ mm/s, $\lambda_0=0.525$ mm, and $\lambda_1=1.05$ mm one obtains a velocity of the shock front of $c_s=0.069$ mm/s. This is in good agreement with the value 0.074 mm/s obtained from a calculation using Eqs. (3) and (7) or Eqs. (4) and (7). A direct evaluation of the shock front velocity from Fig. 2 yields a value of 0.076 mm/s.

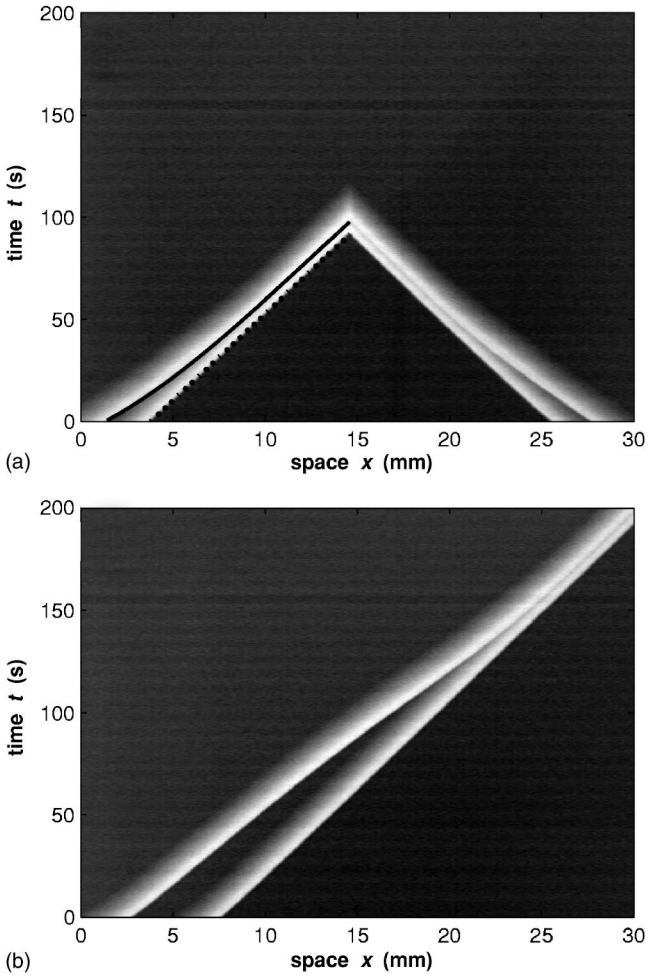

FIG. 4. Space-time plots of consecutive waves with initial wavelengths λ_i on either side of the maximum of the dispersion relation (cf. λ_{max} in Fig. 1). (a) Two wave pairs propagating in opposite direction with $\lambda_i = 2.5$ mm ($dC/d\lambda > 0$) and an annihilation process at $t \approx 100$ s. The dotted line indicates the linear behavior of the first front. The solid line indicates the trajectory obtained from Eq. (4). (b) With $\lambda_i = 5.1$ mm the wave starts at the anomalous branch ($dC/d\lambda < 0$) of the dispersion curve. Initial concentrations are the same as in Fig. 2 except $[NaBrO_3] = 0.15$ M.

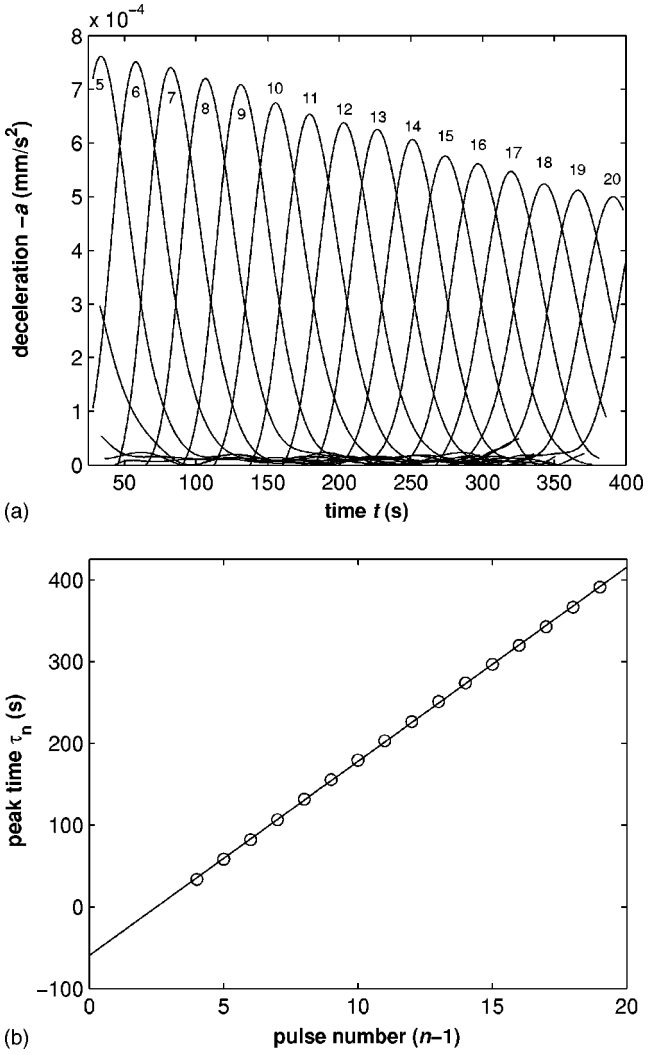

FIG. 5. (a) Deceleration $-a_n$ as a function of time for several consecutive pulses. The small numbers below and above the peaks denote the pulse numbers n. (b) Corresponding peak times τ_n as a function of the pulse number $(n-1)$ (open circles). The solid line is the best linear fit. Its inverse slope is 0.042 s^{-1}.

A mild discrepancy between our experimental data and Eq. (7) is discussed in the following. According to Eq. (7), we expect the intercept of the regression line ($\tau = -60$ s) to approximate the initiation time of the first pulse ($n = 0$). Because early initiation events are not captured in the measurement, we approximate the initiation time by linear extrapolation of the leading pulse trajectory in Fig. 2. This analysis suggests initiation at −91 s. The latter value is surprisingly smaller than the τ intercept of −60 s in Fig. 5(b). We attribute this difference to increased front velocities in close vicinity of the pacemaker.

Next, we compare the inverse slope of the data in Fig. 5(b) with the dispersion relation of the system. Figure 6 shows the normal branch of the dispersion relation as obtained from a stacking pulse in Fig. 2. In this experiment the linearized slope around λ_0 is 0.36 s^{-1} (dashed line). Linear regression of the entire curve yields 0.049 s^{-1} (solid line). The latter value is in good agreement with the inverse slope (0.042 s^{-1}) of the data in Fig. 5(b). Hence the main features of our theoretical analysis [cf. Eq. (7)] are recovered, but the underlying ν value is approximately the average slope of the dispersion curve over the relevant pulse distance interval.

V. CONCLUSIONS

In conclusion, we have presented a kinematic analysis of stacking and destacking waves in excitable reaction-diffusion systems with anomalous dispersion. Our analysis is based on the linear approximation of the nonmonotonic dispersion relation around the stacking distance λ_0. It yields a rigorous expression [Eq. (3)] for pulse trajectories in arbitrary wave trains for which the initial front positions are known. The applicability of the latter expression to experimental data is successfully demonstrated for chemical waves in the CHD-BZ reaction even if the normal branch of the real dis-

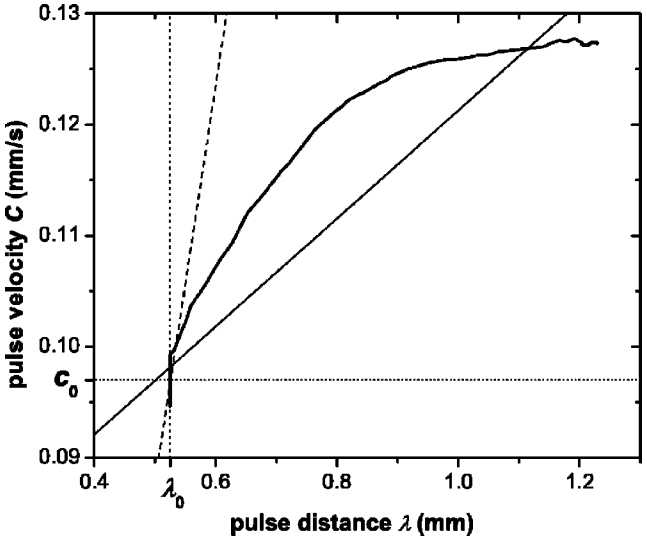

FIG. 6. The normal branch of the dispersion relation as determined from a stacking front in Fig. 2. The solid line represents the best linear fit using all data (slope of 0.049 s^{-1}). The dashed line (slope of 0.36 s^{-1}) is the linear approximation of the $C(\lambda)$ values around λ_0.

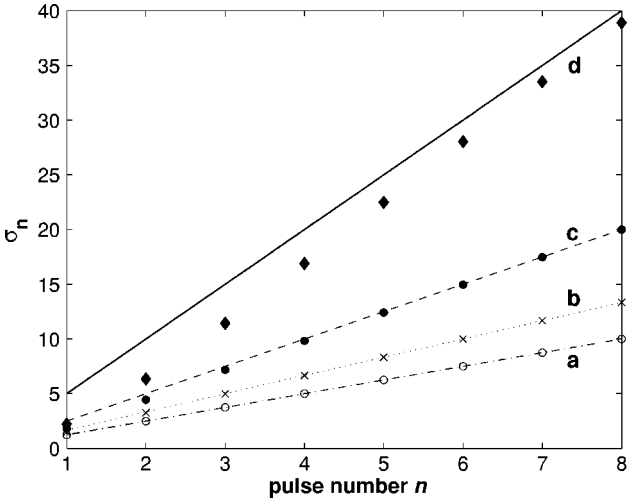

FIG. 7. Evaluation of the usefulness of Eq. (A4) for the analysis of pulses generated by a periodic pacemaker. The discrete values obtained from Eqs. (A1) and (A2) and the continuous approximation in Eq. (A4) are represented by symbols and lines, respectively. The symbol-curve pairs (a–d) correspond to calculations carried out for $\nu T=0.2$ (open circles, dash-dot line), 0.4 (crosses, dotted line), 0.6 (solid circles, dashed line), and 0.8 (solid diamonds, solid line).

persion relation differs from the linearized assumption.

For wave trains in which the front positions are equally spaced at $t=0$, we obtain analytical functions that describe the front velocities and accelerations as a function of time. In particular, kinematic analysis predicts a unique deceleration maximum for each pulse with $n>1$. For subsequent pulse pairs these maxima occur with a lag time equal to the inverse slope $1/\nu$ of the linearized dispersion curve. This simple dependence is reproduced in our experiments.

Last, we emphasize that the results of this study are not limited to the description of excitation waves in chemical and biological reaction-diffusion media. Our results should be also useful for the description of step defects on crystal surfaces and the related analysis of step bunching which constitutes a severe and interesting problem in the field of crystal growth [32]. Moreover, we believe that our findings provide insights into the emergence of traffic jams where individual vehicles interact according to rules that are similar to those dictated by anomalous dispersion relations.

ACKNOWLEDGMENTS

This work was supported by the National Science Foundation (NSF Grant No. CHE-20023105). N.M. thanks the "Deutsche Akademie der Naturforscher Leopoldina" (Grant No. BMBF-LPD 9901/8-85) for financial support. We thank Thomas M. Fischer for discussions.

APPENDIX

In the following, we provide a theoretical description of pulses triggered by a resting, pointlike pacemaker of constant period T. Without loss of generality we assume that the pacemaker is located at $x=0$ and that the frontier pulse $(n=0)$ is triggered at time $t=0$. These assumptions imply that $x_n(nT)=0$ and allow us to determine the integration constants s_n in Eq. (3) from the recursion equation

$$\sigma_1 = e^{\nu T}, \tag{A1}$$

$$\sigma_n = ne^{n\nu T} - \sum_{i=1}^{n-1} \frac{(n\nu T)^i}{i!}\sigma_{n-i}, \tag{A2}$$

and

$$s_n = \sigma_n c_0(T_0 - T) - nc_0T_0, \tag{A3}$$

where $T_0=\lambda_0/c_0$ denotes the period in stacked pulse trains.

Recursive Taylor expansion of Eq. (A2) around $n=0$ suggests that σ_n can be approximated by a geometric series yielding

$$\sigma_n \approx \frac{n}{1-\nu T}. \tag{A4}$$

We find that the latter equation yields very good agreement with Eq. (A2), if $\nu T \ll 1$. For larger values of νT, however, the approximation in Eq. (A4) fails and overestimates σ_n for small n. Figure 7 illustrates this finding for values of νT between 0.2 and 0.8.

Using the approximation given in Eq. (A4), we obtain a simple expression for the integration constants s_n. Substitution of the latter expression into Eq. (3) yields the position and, consequently, the velocity and the acceleration of the nth pulse as a function of time. The resulting equations are identical to those in Eqs. (4)–(6) and (8) if the term $(\lambda - \lambda_0)$ is replaced by $c_0(T_0-T)/(1-\nu T)$. Furthermore, we fully recover Eq. (7) that described the time at which the acceleration reaches an extremum.

[1] M. C. Cross and P. C. Hohenberg, Rev. Mod. Phys. **65**, 851 (1993); *Chemical Waves and Patterns*, edited by R. Kapral and K. Showalter (Kluwer, Dordrecht, The Netherlands, 1995); J. D. Murray, *Mathematical Biology*, 3rd Ed. (Springer, New York, 2002).
[2] N. G. Publicover and K. M. Sanders, J. Physiol. (London) **371**, 179 (1986); R. J. Stevens, J. S. Weinert, and N. G. Publicover, Am. J. Physiol.: Cell Physiol. **277**, C448 (1999).
[3] V. I. Koroleva and J. Bureš, Brain Res. **173**, 209 (1979).
[4] R. A. Gray, A. M. Pertsov, and J. Jalife, Nature (London) **392**, 75 (1998).
[5] J. Lechleiter, S. Girard, E. Peralta, and D. Clapham, Science **252**, 123 (1991).
[6] A. N. Zaikin and A. M. Zhabotinsky, Nature (London) **225**, 535 (1970).
[7] S. Jakubith, H. H. Rotermund, W. Engel, A. von Oertzen, and G. Ertl, Phys. Rev. Lett. **65**, 3013 (1990).
[8] F. Siegert and C. J. Weijer, J. Cell. Sci. **93**, 325 (1989).
[9] K. Krischer, in *Modern Aspects of Electrochemistry, Number 32*, edited by B. E. Conway, J. O'M. Bockris, and R. E. White (Kluwer Academic/Plenum Publishers, New York, 1999), pp. 1–142; K. I. Agladze, S. Thouvenel-Romans, and O. Steinbock, J. Phys. Chem. A **105**, 7356 (2001).
[10] T. Mair and S. C. Müller, J. Biol. Chem. **271**, 627 (1996).
[11] J. Tesarik, M. Sousa, and J. Testart, Hum. Reprod. **9**, 511 (1994); L. F. Jaffe and R. Creton, Cell Calcium **24**, 1 (1998).
[12] N. Suzuki, M. Hirata, and S. Kondo, Proc. Natl. Acad. Sci. U.S.A. **100**, 9680 (2003).
[13] R. J. Field and R. M. Noyes, J. Chem. Phys. **60**, 1877 (1974); J. J. Tyson and P. C. Fife, J. Phys. Chem. **73**, 2224 (1980).
[14] P. K. Brazhnik, V. A. Davydov, and A. S. Mikhailov, Theor. Math. Phys. **74**, 300 (1988); V. A. Davydov, V. A. Zykov, and A. S. Mikhailov, Sov. Phys. Usp. **34**, 665 (1991); A. S. Mikhailov and V. S. Zykov, Physica D **52**, 379 (1991).
[15] D. F. Tatterson and J. L. Hudson, Chem. Eng. Commun. **1**, 3 (1973).
[16] O. Steinbock and S. C. Müller, Physica A **188**, 61 (1992); J.-M. Flesselles, A. Belmonte, and V. Gáspár, J. Chem. Soc., Faraday Trans. **94**, 851 (1998).
[17] J. Christoph, M. Eiswirth, N. Hartmann, R. Imbihl, I. Kevrekidis, and M. Bär, Phys. Rev. Lett. **82**, 1586 (1999).
[18] V. K. Vanag and I. R. Epstein, Phys. Rev. Lett. **88**, 088303 (2002).
[19] N. Manz, S. C. Müller, and O. Steinbock, J. Phys. Chem. A **104**, 5895 (2000).
[20] C. T. Hamik, N. Manz, and O. Steinbock, J. Phys. Chem. A **105**, 6144 (2001).
[21] M. Goldermann, W. Hanke, A. C. Guimaraes de Almeida, and V. M. Fernandes de Lima, Int. J. Bifurcation Chaos Appl. Sci. Eng. **8**, 1541 (1998).
[22] F. Siegert and C. J. Weijer, J. Cell. Sci. **93**, 325 (1989); C. van Oss, A. V. Panfilov, P. Hogeweg, F. Siegert, and C. J. Weijer, J. Theor. Biol. **181**, 203 (1996).
[23] N. Manz, C. T. Hamik, and O. Steinbock, Phys. Rev. Lett. **92**, 248301 (2004); N. Manz and O. Steinbock, J. Phys. Chem. A **108**, 5295 (2004).
[24] D. Helbing, Rev. Mod. Phys. **73**, 1067 (2001).
[25] L. N. Howard and N. Kopell, Stud. Appl. Math. **56**, 95 (1977).
[26] C. T. Hamik and O. Steinbock, Phys. Rev. E **65**, 046224 (2002).
[27] C. T. Hamik and O. Steinbock, New J. Phys. **5**, 58 (2003).
[28] K. Kurin-Csörgei, I. Szalai, I. Molnár-Perl, and E. Körös, React. Kinet. Catal. Lett. **53**, 115 (1994); I. Szalai, E. Körös, and L. Györgyi, J. Phys. Chem. **102**, 6892 (1999).
[29] V. S. Zykov, *Simulations of Wave Processes in Excitable Media* (Manchaster University Press, New York, 1979); A. S. Mikhailov, V. A. Davydov, and V. S. Zykov, Physica D **70**, 1 (1994); V. S. Zykov, O.-U. Kheowan, O. Rangsiman, and S. C. Müller, Phys. Rev. E **65**, 026206 (2002).
[30] K. Kurin-Csörgei, A. M. Zhabotinsky, M. Orbán, and I. R. Epstein, J. Phys. Chem. **100**, 5393 (1996).
[31] W. J. M. Rankine, Philos. Trans. R. Soc. London **160**, 277 (1870); H. Hugoniot, C. R. Hebd. Seances Acad. Sci. **101**, 1118 (1885).
[32] F. C. Frank, in *Growth and Perfection of Crystals*, edited by R. H. Doremus, B. W. Roberts, and D. Turnbull (Wiley, New York, 1958), pp. 411–419; D Kandel and J. D. Weeks, Phys. Rev. Lett. **69**, 3758 (1992).